

Joint Debiased Representation and Image Clustering Learning with Self-Supervision

Shunjie-Fabian Zheng^{1*}, JaeEun Nam^{1*}, Emilio Dorigatti¹, Bernd Bischl¹, Shekoofeh Azizi^{2†}, Mina Rezaei^{1 †}

¹ Department of Statistics, LMU Munich, Germany

² Google Research, Brain Team, Canada

Abstract

Contrastive learning is among the most successful methods for visual representation learning, and its performance can be further improved by jointly performing clustering on the learned representations. However, existing methods for joint clustering and contrastive learning do not perform well on long-tailed data distributions, as majority classes overwhelm and distort the loss of minority classes, thus preventing meaningful representations to be learned. Motivated by this, we develop a novel joint clustering and contrastive learning framework by adapting the debiased contrastive loss to avoid under-clustering minority classes of imbalanced datasets. We show that our proposed modified debiased contrastive loss and divergence clustering loss improves the performance across multiple datasets and learning tasks. The source code is available at <https://anonymous.4open.science/r/SSL-debiased-clustering>

1. Introduction

Self-supervised learning (SSL) has achieved superior performances and outperformed supervised learning models in different research areas such as computer vision [8, 7], natural language processing [13], and more recently medical image analysis [1, 2, 51] and bio-informatics [20]. SSL algorithms learn representations from large scale unlabeled data by solving a *pretext task* such as solving jigsaw puzzles [37], predicting geometric transformations [21], Bregman divergence learning [45], predicting reverse-complement of genome sequences [20], the relative positioning of patches [15], etc. The representations learned by performing such task can then be used as a starting point for different *downstream* tasks such as classification [54], semi-supervised learning [3], clustering [40], or image generation [25]. The performance of self-supervised learning was recently further improved by contrastive methods that train a network to maximize the similarity of representation obtained from different augmented views of the same image [24, 38, 22, 7, 8].

Recent studies have shown that self-supervised pretext task learning benefits from multi-task learning [16, 42] such as performing clustering on the learned representations [58]. However, in spite of the explicit clustering, representations learned in such a way could still exhibit overlap between different classes, particularly for complex datasets with a large number of categories and long-tailed data distribution [31]. There are three reasons underlying this phenomenon. First, [10] showed how the representations induced by traditional contrastive learning are inherently biased as each augmentation is contrasted against *all* other samples in the batch, including potentially those of the same underlying latent class. Second, clustering techniques based on euclidean metrics such as K-means [33] or Gaussian mixture models [6] struggle when operating on data lying on high-dimensional manifolds [26, 43, 49]. Finally, especially in imbalanced datasets, the loss of samples belonging to minority classes is distorted when their representations are contrasted with an excessive number of negative samples from other classes. This limits the learning signal to the network and prevents it from assigning similar representations to minority samples while keeping them sufficiently distinct from those of all the other samples.

In this paper, we thus improve simultaneous clustering and contrastive representation learning for imbalanced datasets by generalizing the debiased contrastive loss of [10] to avoid under-clustering minority classes. An excessive amount of negative samples forces the formation of different clusters within the same category [55], therefore we modified that loss with a smoothing terms that controls the influence of the contrasted negative samples, preventing the previously mentioned phenomenon of under-clustering. We then use these representations to directly perform clustering [57]. Our main contributions can be summarized as:

- We propose a joint framework for self-supervised learning of visual representations and image clustering. Our proposed method learns debiased contrastive visual representation and unsupervised clustering using divergence loss over the data distributions.
- We show empirical results to highlight the benefits of

*Equal Contributions.

†mina.rezaei@stat.uni-muenchen.de, shekazizi@google.com

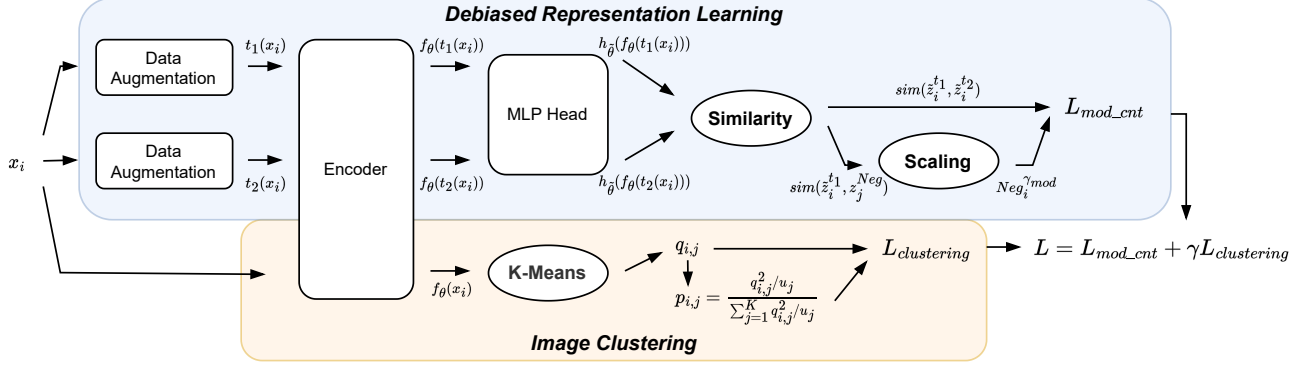


Figure 1. Illustration of the proposed unsupervised debiased representation learning framework. Our method is composed of two parallel deep convolutional transformer architecture where the clustering network takes an original images and the representation network takes two augmented views of the image. The representation network first projects the augmented views onto an embedding space and then processes these representations in a MLP head, which generates the baseline for the pair-wise contrastive objective. Here, we scale the negative sampling strategy of [10] by exponential weighting in order to create an excess of debiased negative samples that leads to under-clustering. The clustering network uses the extracted features from the encoder and employ a K-Means clustering with a KL-divergence loss with the students t-distribution as the soft assignments and a target distribution, as a function of the soft assignments citexie2016unsupervised.

avoiding under-clustering while learning representations using a multi-task learning loss. The model is able to distinguish distinct classes better or at least comparable to the state-of-the-art methods for several benchmark datasets and public medical datasets, characterized by long tailed distributions. Our method is evaluated in linear, semi-supervised, and unsupervised clustering settings on public datasets, achieving comparable or higher performance in comparison to state-of-the-art contrastive learning methods in several tasks.

2. Related Work

Self-supervised Learning Self-supervised learning methods have made a great impact in recent years. Initial studies in self-supervised representation learning focused on the problem of learning embeddings without labels such that a linear classifier on the learned embeddings could achieve competitive accuracy as supervised models [15, 44, 46]. Furthermore, the trained embeddings are also transferable to other tasks. Early methods explore the inter-class structure of the data during pretraining task by generating the masked tokens [13] and future tokens [41] over denoising corruptions [30] to the prediction of the colorization of images [59]. In this sense SSL tries to substitute the ground-truth semantic labels with a clever use of data augmentation techniques [54, 45], takes replaces of the label signal in a supervised setting in order to solve the pretext task. These augmentations range from colorization [59], over rotational predictions [19] to random cropping [54]. The aim of the supervision via data augmentation (hence the name Self-supervision) is to mimic prior knowledge through linear constraints derived from the data structure itself. Instance-wise contrastive learning treats each data point and its transfor-

mations as a separate class and pulls the embeddings of a same class close to each other, while pushing the embeddings of different classes far away [54]. Hence, contrastive learning can be interpreted as a self-supervised Version of the triplet loss. The primary focus of the research of contrastive losses are grounded in different approaches of generating the positive pairs in vision tasks [7, 54, 45]. Only in the last two years has the perspective changed and [10] approaches the sampling problem of treating random data points as dissimilar, even though they might as well belong to the same class. The correction for same label data points within the regular treatment of such as negative examples culminates to the debiased contrastive loss. [47] introduces a control element to the *hardness* of negative examples, as identifying negative examples close to the decision boundary can improve the training performance. We take the negative sampling strategy of the debiased contrastive loss and introduce under-clustering, which happens in cases of an excessive amount of negative samples.

Unsupervised Image Clustering Unsupervised clustering denotes a set of techniques that has the goal of finding structure within the latent space in order to group data points with similar traits [40]. As real world data is frequently high dimensional as in pixels per image and long texts, unsupervised clustering algorithms conduct a dimensionality reduction, which extracts lower dimensional features from the data with no label information. The learned features in the latent space are then subject to a boundary identification over a similarity metric [50]. Among the most popular partition methods are K-Means, which assumes k different classes and assigns the data points to the class, whose centroid is closest to the data point in the latent space [33]. [54] proposed a

multi-step approach called SCAN, in which high level feature embeddings are generated by representation learning and then used as a baseline for the subsequent clustering task via nearest neighbors. Following SCAN [40] developed the so-called RUC algorithm [40], whereby an add on module is used on top of a generic unsupervised clustering method in order to improve the performance. It is first assumed that the clustering results are noisy as assigned labels can be false. The correctly assigned data points are selected to form a labeled dataset while the other samples are considered unlabeled, which allows the subsequent network to learn in a semi supervised manner with label smoothing[36]. Most recently, SPICE [36] was proposed, an algorithm consisting of two semantic aware pseudo labeling networks to allow for reliable self supervision via self-labeling and the extraction of semantically crucial features reflecting the ground truth.

3. Method

Fig. 1 shows our proposed method. An encoder is used to learn common representations, which are then processed by two parallel networks: the *representation network* and the *deep divergence clustering network*. The representation network learns representations using our modified debiased contrastive loss, while the clustering network ensures that the learned representations cluster faithfully. Each of these two modules comes with its own loss which is mixed following a parameter γ into the main loss used for training:

$$\mathcal{L}_{MTL} = \mathcal{L}_{deb}^{mod} + \gamma \cdot \mathcal{L}_{clustering} \quad (1)$$

3.1. Image encoding

Before clustering and representation learning, images are encoded to a common representation in an embedding space Z by an encoder f . We used ConvMixer, an isotropic vision model that operates on patches, in order to preserve some local structure within each part of an image [52]. The input image is first divided into patches of size p_s and dimension d_h , which are then fed into series of convolutional mixing blocks consisting of subsequent depth-wise convolutions, in order to mix the spatial structure of the image, and point-wise convolutions, in order to mix channel locations. To this base architecture we added another residual connection from the output of the depth-wise convolution to the output of the point-wise convolution. In this sense, our backbone model differs from [52], as only one residual connection for spatial awareness was used and thus the original ConvMixer possesses only flexibility in regards to the depth of an image. By repeated mixing, stacking mixing blocks, an arbitrary large receptive field can be created as distant spatial structures are mixed together the more mixing blocks are used [52].

3.2. Self-supervised Representation Learning

As shown in Fig. 1, our method takes the original image and creates two augmented views using two random transform functions t_1, t_2 . The augmented views are generated by applying random cropping, resizing and random Gaussian blurs sequentially on an image twice [7], where the resizing is meant to bring the dimensionality of the cropped image back to its input dimensions. The encoder network f then projects a sample image $x_i^{(j)}$ onto the common embedding space before a further MLP head h gives the final representations used with our modified contrastive loss. Previous work [] has shown that performance in downstream tasks benefits from using intermediate representations rather than those directly used for contrastive learning.

Specifically, from an input image x_i we derive two representations $z_i^{(k)} := h(f(t_k(x_i)))$, $k \in \{1, 2\}$, thus generating $2N$ representations from a mini-batch B with cardinality N . For convenience, we group the representations of all samples $j \neq i$ into $\bar{Z}_i = \{z_j^{(k)} | j \neq i, k \in \{1, 2\}\}$. The representation of a sample $z_i^{(k)}$ is contrasted via the cosine-similarity $sim(z_i, z_j) := (z_i^\top z_j)(z_i^\top z_i)^{-1}(z_j^\top z_j)^{-1}$ with temperature τ to the representations of all other samples, defining an average distance:

$$S_i^{(k)} = \frac{1}{|\bar{Z}_i|} \sum_{z \in \bar{Z}_i} \exp(sim(z_i^{(k)}, z)/\tau) \quad (2)$$

Due to the absence of training labels, \bar{Z}_i can contain representations of samples belonging to the same category as sample i , leading to sampling biases in the regular contrastive learning setting. The contrastive loss proposed by [10] solves this problem, but is still vulnerable to the issue of under-clustering of minority classes we discussed in the introduction.

To tackle this problem, we introduce a smoothing term λ that softens the impact of the distance D_i of the representations of sample i with those in \bar{Z}_i :

$$\mathcal{L}_{deb,i}^{mod} = -2 \log \frac{\exp(sim(z_i^{(1)}, z_i^{(2)})/\tau)}{\exp(sim(z_i^{(1)}, z_i^{(2)})/\tau) + (1 + D_i)^\lambda} \quad (3)$$

where

$$D_i = \sum_{k=1}^2 \max \left\{ \exp(-1/\tau), \frac{1}{1 - \tau^+} \left(S_i^{(k)} - \tau^+ \exp(sim(z_i^{(1)}, z_i^{(2)})) \right) \right\}$$

and τ^+ is the prior probability that a sample belongs to the same class of x . Through λ we control the emphasis on under-clustering, since an excessive amount of negative samples forces the formation of different clusters within the

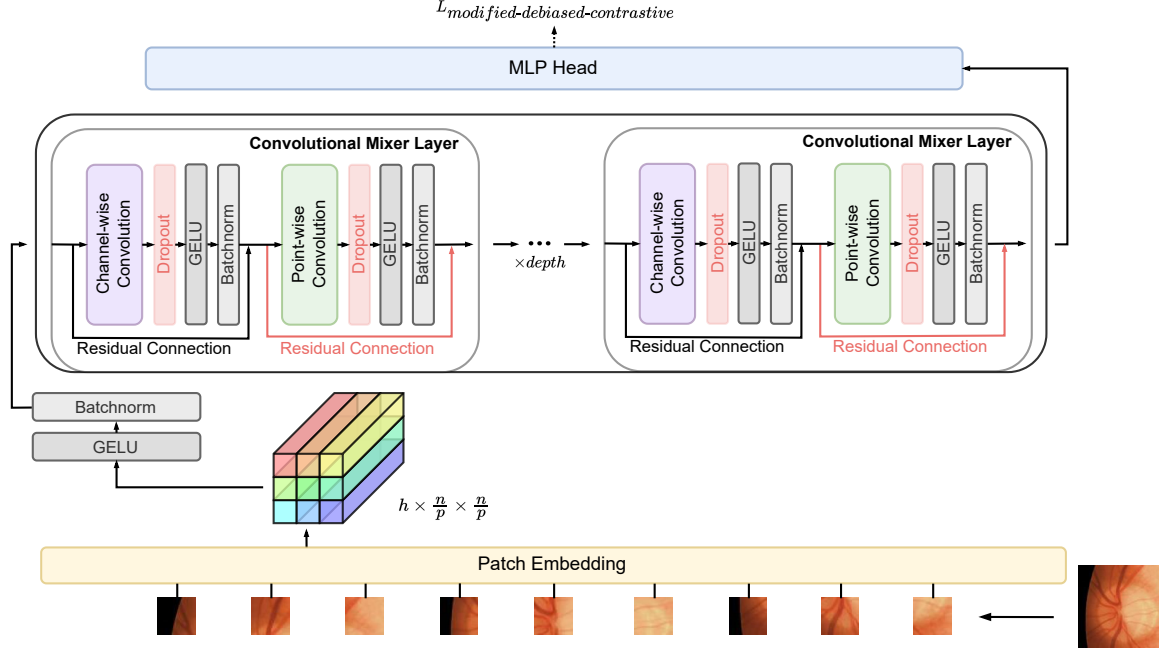


Figure 2. Illustration of the encoder architecture based on ConvMixer [53]. First an input image is divided into relatively small patches which are then processed in mixing layers, consisting of subsequent channel-wise and point-wise convolutions. In contrast to the original ConvMixer the convolutions are followed by a dropout layer in order to prevent over-fitting and to extract more salient features. Following the idea of residual networks [23] we added another residual connection (in red) to enable the point-wise convolution more flexibility during training and to increase the hypothesis space even further. Applying consecutive mixing layers allows the encoder to learn the global structure of the images and can be seen as a form of self attention.

same category [55], thereby tackling the problem of *within cluster imbalance*.

Applying Eq. 3 on a mini-batch B results in the loss for the representation learning network:

$$\mathcal{L}_{deb}^{mod} = \frac{1}{2N} \sum_{i=1}^N \mathcal{L}_{deb,i}^{mod} \quad (4)$$

3.3. Self-Supervised Debiased Clustering

The purpose of the clustering network is to refine and improve the learned contrastive representations such that they cluster properly. We assume that the dataset consists of a long tailed distribution of images over a known number of K categories. The clustering is refined by pushing the soft label assignments q_{ij} towards the target distribution P by matching them via KL-divergence [57]:

$$\mathcal{L}_{clustering} = KL(P||Q) = \sum_{i=1}^N \sum_{j=1}^K p_{ij} \log \frac{p_{ij}}{q_{ij}} \quad (5)$$

The embeddings $z_i := f(x_i)$ generated by the encoder are subject to a K -Means clustering algorithm, where the similarity of an embedded image to the cluster center μ_j ,

with $j \in K$ is measured by the Student's t-distribution [32]:

$$q_{ij} = \frac{(1 + \|z_i - \mu_j\|_2^2 / \alpha)^{-\frac{\alpha+1}{2}}}{\sum_{l=1}^K (1 + \|z_i - \mu_l\|_2^2 / \alpha)^{-\frac{\alpha+1}{2}}} \quad (6)$$

Where α denotes the degree of freedom and will be set to 1 throughout [32]. The cluster centers are initialized by performing standard K-Means clustering on the embeddings [57]. Raising the soft label assignments q_{ij} to the second power and normalizing it by the cluster frequencies $u_j = \sum_{i=1}^N q_{i,j}$ generates an auxiliary target distribution P for self-supervision [57]. The single elements of P can be computed by:

$$p_{ij} = \frac{q_{ij}^2 / u_j}{\sum_{j=1}^K q_{ij}^2 / u_j} \quad (7)$$

p_{ij} sharpens q_{ij} and due to the normalization reduces bias from imbalanced clusters, while forced to learn the soft label assignments with high confidence [58].

4. Implementation

We train our framework for multiple pretext tasks learning. We follow standard protocols by self-supervised learning for empirical analysis and evaluate the learned representation of our model by classification, semi-supervised,

as well as image clustering tasks on different datasets and different computer vision tasks.

Datasets and tasks We consider a group of standard datasets in two scenarios. First, relatively balanced data, and secondly, imbalanced setting. For the balanced settings, we used CIFAR-10 [29], CIFAR-100 [29], and Glaucoma-1, which is the labeled subset of the collection of human retinal images used by [14]. This dataset is composed of 2,397 samples where 956 are diagnosed with glaucoma, and 1421 with no-glaucoma.

For the imbalanced analysis, we performed our experiments on imbalanced CIFAR-10/100 and Glaucoma-2 [39]. We followed the suggested setting by Cao et al. [5] for the imbalanced CIFAR10/100 in the long-tailed setting and 1:100 as an imbalanced ratio. The Glaucoma-2 contains retina microscopic images in two classes of healthy and Glaucoma with an imbalanced ratio of 1:9. The dataset was released at the REFUGE-2 challenge [39], part of MICCAI conference 2020/21. The ISIC-2018 dataset was released at MICCAI 2018 as a challenge dataset and it contains 7 different skin lesions where the imbalance ratio is 1:1:3:5:10:11:69.

Image augmentation Similar to SimCLR [7], the random transformation function T applies a combination of image cropping, color jittering, grayscale, horizontal flip, and Gaussian blur. We apply crops with a random size ranging from 0.08 to 1.0 of the original area and a random aspect ratio from $3/4$ to $4/3$ of the original aspect ratio. The cropped part is then resized to the original size. We also apply horizontal flipping with a probability of 0.5 and apply grayscale with a probability of 0.2 as well as color jittering with a probability of 0.8 and a configuration of (0.4, 0.4, 0.4, 0.1). Gaussian blur is applied with a kernel size of 10% of the original image size, a σ randomly sampled from [0.1, 2.0], and a probability of 0.5.

Deep debiased representation architecture First the encoder takes an input image and divides it into quadratic patches of size p . These patches are then fed into a sequence of d Convolutional Mixer Layers which consist of two types of separable convolutions: depth-wise convolutions and point-wise convolution. Here, we modified the supervised ConvMixer architecture [53] 1) by making a network self-supervised, 2) adding a new residual connection in order to create further flexibility for the depth awareness of the network, and 3) adding the dropout layers. As depicted in Fig. 2, the Convolutional Mixing Layers contain channel-wise followed by point-wise convolutions. After each convolution a dropout layer is implemented with a dropout rate followed by a GELU activation layer (Gaussian error linear unit) and a batch normalization. Moreover, each convolution is endowed with corresponding residual connections. Finally, the embeddings are generated by a linear projection of the last Convolutional Mixing Layer.

The experiment is conducted on $p = 2$ pixel patches and

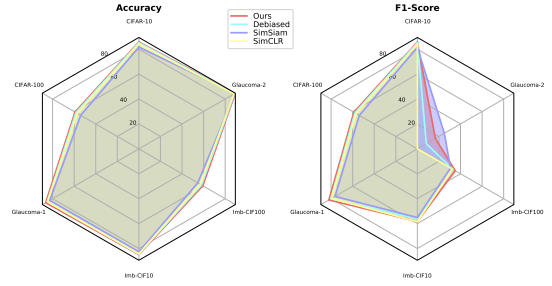


Figure 3. Comparison of the proposed method with baselines under linear evaluation measured by top-1 accuracy (Left) followed by F1-score (Right).

$d = 8$ mixing blocks. Both convolutions have an equal number of channels with 256. The depth-wise convolution uses a kernel size of 7. The linear projection contains two fully connected layers. The first one projects onto 512 hidden neurons and the second projects onto a 128 dimensional embedding space.

We also train our deep unsupervised clustering network with the same architecture as described above (see Fig. 1).

Optimization Following [10], we used the Adam optimizer [28] with a learning rate of 10^{-3} , $\beta_1 = 0.9$, $\beta_2 = 0.999$, and a weight decay of 10^{-6} . Accordingly, the temperature hyperparameter τ was set to 0.5 and the positive class prior τ^+ to 0.1. The emphasis on negative samples γ_{mod} and the weight of the clustering loss γ were set to 2 and 5, respectively. They were tuned by grid search on $\{(\gamma, \gamma_{mod}) : \gamma \in \{0.1, 1, 5\}, \gamma_{mod} \in \{2, 3, 5\}\}$. We chose a dropout rate of 0.04 and different mini-batch sizes depending on the image size. For CIFAR-10/-100, we used a size of 256 and for the medical datasets a size of 32. All the models were trained for 500 epochs on a single GPU (Tesla A100) with 40 GB of memory.

5. Experiments and Results

Linear Evaluation Following the standard linear evaluation protocol [7, 10], the representations of the backbone network were fixed and the projection head was removed after training. Then, a linear classifier on top was trained using the cross entropy loss for 100 epochs with a batch size of 512. Table 1 shows the achieved performance on relative balanced dataset. Considering the imbalance in datasets, we report the Binary or Macro F1-score depending on the number of classes, in addition to the top-1 accuracy on the respective testing sets in Table 2 and Fig. 3.

Semi-Supervision For testing the models in a semi-supervised scenario, we train the linear classifier using only 10% of the training data. Table 3, 4, and Figure 4 shows the top-1 accuracy and the F1-score for balanced and imbalanced dataset respectively.

Table 1. Comparison of the proposed method with baselines under linear evaluation on relatively balanced dataset and measured by top-1 accuracy (%) and F1-score, respectively.

Method	Glaucoma-1	CIFAR-10	CIFAR-100
SimCLR [7]	84.86 \pm 1.37/79.63 \pm 1.80	84.20 \pm 0.06 /84.03 \pm 1.4	57.15 \pm 0.11/56.84 \pm 0.05
SimSiam [9]	82.64 \pm 0.98 /76.36 \pm 1.77	81.68 \pm 0.57/ 81.45 \pm 0.59	53.93 \pm 0.40 /53.8 \pm 0.43
Debiased [10]	84.86 \pm 0.20/80.22 \pm 0.30	85.19 \pm 0.41 /85.09 \pm 0.39	58.32 \pm 0.55 /57.85 \pm 0.63
Our method	86.39 \pm 0.40 /81.99 \pm 0.15	85.74 \pm 0.34 /85.64 \pm 0.29	59.18 \pm 0.37/58.83 \pm 0.49

Table 2. Comparison of the proposed method with baselines on imbalanced dataset under linear evaluation measured by top-1 accuracy (%) and F1-score, respectively.

Method	Glaucoma-2	Imb-CIFAR 10	Imb-CIF100
SimCLR [7]	88.39 \pm 0.96 /0.00 \pm 0.5	84.26 \pm 0.34/58.46 \pm 0.44	56.95 \pm 1.10/32.60 \pm 1.03
SimSiam [9]	89.04 \pm 0.91 /23.02 \pm 1.43	82.69 \pm 0.17 /55.17 \pm 0.08	54.62 \pm 0.59/30.75 \pm 0.33
Debiased [10]	88.89 \pm 0.92/27.07 \pm 4.3	84.47 \pm 0.91 /56.14 \pm 0.14	58.03 \pm 0.43/33.08 \pm 0.53
Our method	89.44 \pm 0.18/60.17 \pm 0.3	84.85 \pm 0.83/58.33 \pm 2.77	59.22 \pm 1.33/35.12 \pm 1.20

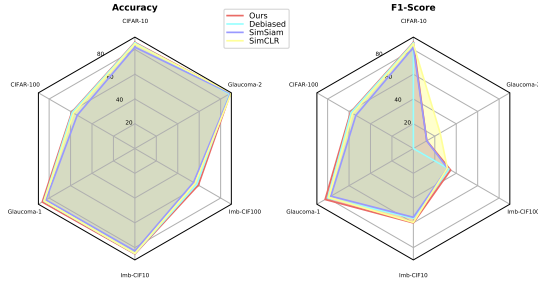


Figure 4. Comparison of the proposed method with baselines under semi-supervised evaluation measured by top-1 accuracy (Left) followed by F1-score (Right).

Unsupervised Clustering Clustering is examined by running the K-Nearest Neighbor algorithm (KNN) with the features of the pretrained encoder. We use a relatively small neighborhood size of 20, considering possible small classes in imbalanced datasets, and report the outcomes in Table 5.

6. Ablation Study

We further investigate the following aspects of our approach in multiple ablation analysis: (1) analysis of clustering loss and hyperparameters, (2) the impact of modified ConvMixer networks, and (3) robustness of our algorithm for training on imbalanced data distribution.

Network architecture We consider different network architecture as an encoder architecture such as ResNet-18 [23] and CoAtNet [12]. ResNet-18 composed of the 17 convolutional layers [23] and it addressed the problem of vanishing gradients in deep networks by residual connections. The network learns the identify function of the previous convolutional layer, which makes the training of deep convolutional neural networks (CNN) more efficient and gives the ability

to compress the model, reducing the need for neural architecture search. CoAtNet unites depth-wise convolution and relative self attention [12]. The main idea is to keep the desirable properties such as the generalizability of CNNs and the high model capacity of transformers. This is achieved by stacking convolutional and transformer blocks. The convolutional block consisting of an expansion, depth-wise convolution and following compression to the input size. The Transformer block starts with a relative attention layer, which can be skipped through a residual connection same as the whole convolutional block and a subsequent multi layer perceptron. The input image is divided into patches to enable global attention-[17] and then fed into a combination of stacked convolutional and transformer blocks before being projected by a fully connected layer. Table 6 shows and compares the impact of encoder architecture.

Clustering We examine Clustering was performed with the K-Nearest Neighbor algorithm (KNN). We used a neighborhood size of 20 and report the top-1 accuracy and the (Binary / Macro) F1-score in Table 5.

Robustness against imbalanced data distribution Since the success of deep learning methods in a variety of downstream task on balanced data, researchers steadily shifted their focus on solutions for imbalanced data problems, as they are a more accurate portray of real world data [56]. In a supervised setting, the problem can be tackled by the use of data balancing techniques such as down sampling the majority class [4, 18] or up sampling the infrequently observed classes [4, 48], both of which aims to produce a more balanced data set during the training process [34]. The effectiveness of data balancing is intuitively given, nevertheless, it has to be said that those methods come with their own set of downsides. down sampling can lead to a loss of information within the majority class and up sampling brings the risk of over-fitting the minority class, as no

Table 3. Comparison of the proposed method with baselines on balanced dataset under semi-supervised evaluation measured by top-1 accuracy (%) and F1-score, respectively.

Method	Glaucoma-1	CIFAR-10	CIFAR-100
SimCLR [7]	84.59 \pm 0.98/79.10 \pm 1.27	84.50 \pm 0.69/84.37 \pm 0.69	57.18 \pm 0.28/56.67 \pm 0.30
SimSiam [9]	83.06 \pm 0.00/76.97 \pm 0.74	81.88 \pm 0.42/81.71 \pm 0.42	53.80 \pm 0.52/53.63 \pm 0.54
Debiased [10]	84.86 \pm 1.37/79.77 \pm 1.99	85.27 \pm 0.37/85.14 \pm 0.39	58.41 \pm 0.18/58.11 \pm 0.23
Our method	86.30 \pm 1.17/82.32 \pm 1.26	85.72 \pm 0.41/85.62 \pm 0.43	58.82 \pm 0.01/58.63 \pm 0.13

Table 4. Comparison of the proposed method with baselines on imbalanced dataset under semi-supervised evaluation measured by top-1 accuracy (%) and F1-score, respectively.

Method	ISIC	Glaucoma-2	Imb-CIF10	Imb-CIF100
SimCLR [7]	68.55 \pm 0.04/38.62 \pm 0.00	88.00 \pm 0.00/55.00 \pm 0.00	84.77 \pm 0.14/59.71 \pm 0.64	56.25 \pm 0.63/31.70 \pm 0.34
SimSiam [9]	61.31 \pm 0.08/31.21 \pm 0.01	89.17 \pm 1.18/42.50 \pm 17.68	82.75 \pm 0.14/55.56 \pm 3.73	54.74 \pm 1.23/31.83 \pm 1.47
Debiased [10]	62.43 \pm 0.05/33.11 \pm 0.00	88.33 \pm 0.00/52.06 \pm 0.00	84.79 \pm 0.11/56.34 \pm 3.73	57.79 \pm 0.76/33.20 \pm 0.21
Our method	73.29 \pm 0.04/67.12 \pm 0.01	89.19 \pm 1.18/72.50 \pm 0.68	85.17 \pm 0.48/60.09 \pm 1.41	59.20 \pm 0.37/34.79 \pm 0.43

Table 5. Comparison of the proposed method with the baseline on image clustering measured by top-1 accuracy (%) and F1-score.

Method	ISIC	Glaucoma-1	Glaucoma-2	CIFAR-10	Imb-CIFAR-10	CIFAR-100	Imb-CIFAR-100
SimCLR [7]	48.50/14.46	81.17/80.41	90.00/40.00	78.11/77.97	79.18/49.63	47.84/47.78	45.38/27.14
SimSiam [9]	47.64/14.35	80.83/76.45	86.67/33.33	75.21/75.17	74.82/46.70	43.01/42.79	41.30/23.23
Debiased [10]	47.70/14.55	83.33/79.45	93.33/60.00	80.70/80.59	80.31/50.37	49.08/49.01	46.03/25.75
Our method	49.30/15.42	84.50/78.05	96.32/68.36	80.93/80.86	81.51/63.43	49.89/49.09	46.50/25.52

Table 6. Top-1 accuracy (%) and F1 score for image clustering evaluation where all the networks are trained with our proposed loss function.

Encoder/dataset	CIFAR10	CIFAR100	Imb-CIF-10	Imb-CIF-100	Glaucoma-1	Glaucoma-2	ISIC
ResNet	78.66/78.64	56.28/56.42	83.62/67.33	50.07/27.39	84.17/80.81	91.23/46.15	48.30
CoAtNet	74.78/74.66	43.56/43.32	76.92/47.25	41.48/23.10	83.11/80.13	90.0/40.0	50.23
ConvMixer	80.93/80.86	49.89/49.09	81.51/63.43	46.50/25.52	84.50/80.05	96.32/68.36	49.30

more additional information is generated [35]. Other solutions modify the loss function, such that it can be defined as cost sensitive. loss re-weighting techniques puts a higher weight on minority classes and a lower weight on majority classes, effectively [27, 11]. The single re-weighting methods mainly differ in how and what weights are assigned to which class [56].

7. Conclusion

In this paper, we introduce a new self-supervised multi-task learning framework which learns simultaneously unsupervised representation and perform image clustering. We explored a self-supervised embedding trained jointly for clustering and debiased representation learning is more robust for dataset with imbalanced distribution. Moreover, image clustering benefits of this of self-supervised embedding. In this study, we addressed problem of under-clustering which is due to imbalanced distribution by re-designing the previous debiased contrastive loss. Then, networks are optimized end-to-end using our modified debiased contrastive loss and KL-divergence loss. We improved over previous methods for

deep clustering, deep self-supervised, and semi-supervised learning. Empirical experiments demonstrate the efficacy of the proposed method on standard benchmarks as well as imbalanced clinical datasets.

Acknowledgments: We would like to thank Priyank Jaini for valuable feedback on the manuscript. We also would like to acknowledge that E. D. is supported by the Helmholtz Association under the joint research school “Munich School for Data Science - MUDS” (Award Number HIDSS-0006), M. R. and B. B. were supported by the Bavarian Ministry of Economic Affairs, Regional Development and Energy through the Center for Analytics – Data – Applications (ADA-Center) within the framework of BAYERN DIGITAL II (20-3410-2-9-8), and M. R. and B. B. were supported by the German Federal Ministry of Education and Research (BMBF) Munich Center for Machine Learning (MCML).

References

- [1] Shekoofeh Azizi, Laura Culp, Jan Freyberg, Basil Mustafa, Sebastien Baur, Simon Kornblith, Ting Chen, Patricia MacWilliams, S Sara Mahdavi, Ellery Wulczyn, et al. Robust and efficient medical imaging with self-supervision. *arXiv preprint arXiv:2205.09723*, 2022. [1](#)
- [2] Shekoofeh Azizi, Basil Mustafa, Fiona Ryan, Zachary Beaver, Jan Freyberg, Jonathan Deaton, Aaron Loh, Alan Karthikesalingam, Simon Kornblith, Ting Chen, et al. Big self-supervised models advance medical image classification. In *Proceedings of the IEEE/CVF International Conference on Computer Vision*, pages 3478–3488, 2021. [1](#)
- [3] Haoping Bai, Meng Cao, Ping Huang, and Jiulong Shan. Self-supervised semi-supervised learning for data labeling and quality evaluation. *arXiv preprint arXiv:2111.10932*, 2021. [1](#)
- [4] Mateusz Buda, Atsuto Maki, and Maciej A. Mazurowski. A systematic study of the class imbalance problem in convolutional neural networks. 106:249–259. [6](#)
- [5] Kaidi Cao, Colin Wei, Adrien Gaidon, Nikos Arechiga, and Tengyu Ma. Learning imbalanced datasets with label-distribution-aware margin loss. *Advances in neural information processing systems*, 32, 2019. [5](#)
- [6] Gilles Celeux and G  rard Govaert. Gaussian parsimonious clustering models. 28(5):781–793. [1](#)
- [7] Ting Chen, Simon Kornblith, Mohammad Norouzi, and Geoffrey Hinton. A simple framework for contrastive learning of visual representations. In *International conference on machine learning*, pages 1597–1607. PMLR, 2020. [1](#), [2](#), [3](#), [5](#), [6](#), [7](#)
- [8] Ting Chen, Simon Kornblith, Kevin Swersky, Mohammad Norouzi, and Geoffrey E Hinton. Big self-supervised models are strong semi-supervised learners. *Advances in neural information processing systems*, 33:22243–22255, 2020. [1](#)
- [9] Xinlei Chen and Kaiming He. Exploring simple siamese representation learning. In *Proceedings of the IEEE/CVF Conference on Computer Vision and Pattern Recognition*, pages 15750–15758, 2021. [6](#), [7](#)
- [10] Ching-Yao Chuang, Joshua Robinson, Yen-Chen Lin, Antonio Torralba, and Stefanie Jegelka. Debaised contrastive learning. *Advances in neural information processing systems*, 33:8765–8775, 2020. [1](#), [2](#), [3](#), [5](#), [6](#), [7](#)
- [11] Yin Cui, Menglin Jia, Tsung-Yi Lin, Yang Song, and Serge Belongie. Class-balanced loss based on effective number of samples. In *Proceedings of the IEEE/CVF conference on computer vision and pattern recognition*, pages 9268–9277, 2019. [7](#)
- [12] Zihang Dai, Hanxiao Liu, Quoc V Le, and Mingxing Tan. Coatnet: Marrying convolution and attention for all data sizes. *Advances in Neural Information Processing Systems*, 34:3965–3977, 2021. [6](#)
- [13] Jacob Devlin, Ming-Wei Chang, Kenton Lee, and Kristina Toutanova. BERT: Pre-training of deep bidirectional transformers for language understanding. In *Proceedings of the 2019 Conference of the North American Chapter of the Association for Computational Linguistics: Human Language Technologies, Volume 1 (Long and Short Papers)*, pages 4171–4186. Association for Computational Linguistics. [1](#), [2](#)
- [14] Andres Diaz-Pinto, Adri  n Colomer, Valery Naranjo, Sandra Morales, Yanwu Xu, and Alejandro F Frangi. Retinal image synthesis and semi-supervised learning for glaucoma assessment. *IEEE transactions on medical imaging*, 38(9):2211–2218, 2019. [5](#)
- [15] Carl Doersch, Abhinav Gupta, and Alexei A Efros. Unsupervised visual representation learning by context prediction. In *Proceedings of the IEEE international conference on computer vision*, pages 1422–1430, 2015. [1](#), [2](#)
- [16] Carl Doersch and Andrew Zisserman. Multi-task self-supervised visual learning. In *Proceedings of the IEEE international conference on computer vision*, pages 2051–2060, 2017. [1](#)
- [17] Alexey Dosovitskiy, Lucas Beyer, Alexander Kolesnikov, Dirk Weissenborn, Xiaohua Zhai, Thomas Unterthiner, Mostafa Dehghani, Matthias Minderer, Georg Heigold, Sylvain Gelly, et al. An image is worth 16x16 words: Transformers for image recognition at scale. *arXiv preprint arXiv:2010.11929*, 2020. [6](#)
- [18] Chris Drummond, Robert C Holte, et al. C4. 5, class imbalance, and cost sensitivity: why under-sampling beats over-sampling. In *Workshop on learning from imbalanced datasets II*, volume 11, pages 1–8, 2003. [6](#)
- [19] Spyros Gidaris, Praveer Singh, and Nikos Komodakis. Unsupervised representation learning by predicting image rotations. [2](#)
- [20] H  seyin Anil G  nd  z, Martin Binder, Xiao-Yin To, Ren   Mreches, Philipp C M  nch, Alice C McHardy, Bernd Bischl, and Mina Rezaei. Self-genomenet: Self-supervised learning with reverse-complement context prediction for nucleotide-level genomics data. 2021. [1](#)
- [21] Sayed Hashim and Muhammad Ali. Transformnet: Self-supervised representation learning through predicting geometric transformations. *arXiv preprint arXiv:2202.04181*, 2022. [1](#)
- [22] Kaiming He, Haoqi Fan, Yuxin Wu, Saining Xie, and Ross Girshick. Momentum contrast for unsupervised visual representation learning. pages 9729–9738. [1](#)
- [23] Kaiming He, Xiangyu Zhang, Shaoqing Ren, and Jian Sun. Deep residual learning for image recognition. In *Proceedings of the IEEE conference on computer vision and pattern recognition*, pages 770–778, 2016. [4](#), [6](#)
- [24] Olivier Henaff. Data-efficient image recognition with contrastive predictive coding. In *International conference on machine learning*, pages 4182–4192. PMLR, 2020. [1](#)
- [25] Tobias Hinz and Stefan Wermter. Image generation and translation with disentangled representations. In *2018 International Joint Conference on Neural Networks (IJCNN)*, pages 1–8. IEEE, 2018. [1](#)
- [26] Robert C Holte, Liane Acker, Bruce W Porter, et al. Concept learning and the problem of small disjuncts. In *IJCAI*, volume 89, pages 813–818. Citeseer, 1989. [1](#)
- [27] Salman H Khan, Munawar Hayat, Mohammed Bennamoun, Ferdous A Sohel, and Roberto Togneri. Cost-sensitive learning of deep feature representations from imbalanced data. *IEEE transactions on neural networks and learning systems*, 29(8):3573–3587, 2017. [7](#)

- [28] Diederik P Kingma and Jimmy Ba. Adam: A method for stochastic optimization. *arXiv preprint arXiv:1412.6980*, 2014. 5
- [29] Alex Krizhevsky, Geoffrey Hinton, and et al. Learning multiple layers of features from tiny images. 2009. 5
- [30] Mike Lewis, Yinhan Liu, Naman Goyal, Marjan Ghazvininejad, Abdelrahman Mohamed, Omer Levy, Veselin Stoyanov, and Luke Zettlemoyer. BART: Denoising sequence-to-sequence pre-training for natural language generation, translation, and comprehension. In *Proceedings of the 58th Annual Meeting of the Association for Computational Linguistics*, pages 7871–7880. Association for Computational Linguistics, 2020. 2
- [31] Ziwei Liu, Zhongqi Miao, Xiaohang Zhan, Jiayun Wang, Boqing Gong, and Stella X Yu. Large-scale long-tailed recognition in an open world. In *Proceedings of the IEEE/CVF Conference on Computer Vision and Pattern Recognition*, pages 2537–2546, 2019. 1
- [32] Laurens van der Maaten. Learning a parametric embedding by preserving local structure. In *Proceedings of the Twelfth International Conference on Artificial Intelligence and Statistics*, pages 384–391. PMLR, 2017. 4
- [33] J. MacQueen. Some methods for classification and analysis of multivariate observations. 5.1:281–298. 1, 2
- [34] Dhruv Mahajan, Ross Girshick, Vignesh Ramanathan, Kaiming He, Manohar Paluri, Yixuan Li, Ashwin Bharambe, and Laurens Van Der Maaten. Exploring the limits of weakly supervised pretraining. In *Proceedings of the European conference on computer vision (ECCV)*, pages 181–196, 2018. 6
- [35] Ajinkya More. Survey of resampling techniques for improving classification performance in unbalanced datasets. 7
- [36] Chuang Niu and Ge Wang. Spice: Semantic pseudo-labeling for image clustering, 2021. 3
- [37] Mehdi Noroozi and Paolo Favaro. Unsupervised learning of visual representations by solving jigsaw puzzles. In *European conference on computer vision*, pages 69–84. Springer, 2016. 1
- [38] Aaron van den Oord, Yazhe Li, and Oriol Vinyals. Representation learning with contrastive predictive coding. *arXiv preprint arXiv:1807.03748*, 2018. 1
- [39] José Ignacio Orlando, Huazhu Fu, João Barbosa Breda, Karel van Keer, Deepti R Bathula, Andrés Diaz-Pinto, Ruogu Fang, Pheng-Ann Heng, Jeyoung Kim, JoonHo Lee, et al. Refuge challenge: A unified framework for evaluating automated methods for glaucoma assessment from fundus photographs. *Medical image analysis*, 59:101570, 2020. 5
- [40] Sungwon Park, Sungwon Han, Sundong Kim, Danu Kim, Sungkyu Park, Seunghoon Hong, and Meeyoung Cha. Improving unsupervised image clustering with robust learning. In *Proceedings of the IEEE/CVF Conference on Computer Vision and Pattern Recognition*, pages 12278–12287, 2021. 1, 2, 3
- [41] Alec Radford, Karthik Narasimhan, Tim Salimans, Ilya Sutskever, et al. Improving language understanding by generative pre-training. 2018. 2
- [42] Mina Rezaei, Emilio Dorigatti, David Ruegamer, and Bernd Bischl. Learning statistical representation with joint deep embedded clustering. *arXiv preprint arXiv:2109.05232*, 2021. 1
- [43] Mina Rezaei, Emilio Dorigatti, David Ruegamer, and Bernd Bischl. Learning statistical representation with joint deep embedded clustering. *arXiv preprint arXiv:2109.05232*, 2021. 1
- [44] Mina Rezaei, Janne J Näppi, Christoph Lippert, Christoph Meinel, and Hiroyuki Yoshida. Generative multi-adversarial network for striking the right balance in abdominal image segmentation. *International journal of computer assisted radiology and surgery*, 15(11):1847–1858, 2020. 2
- [45] Mina Rezaei, Farzin Soleymani, Bernd Bischl, and Shekoofeh Azizi. Deep bregman divergence for contrastive learning of visual representations. *arXiv preprint arXiv:2109.07455*, 2021. 1, 2
- [46] Mina Rezaei, Haojin Yang, and Christoph Meinel. Generative adversarial framework for learning multiple clinical tasks. In *2018 Digital Image Computing: Techniques and Applications (DICTA)*, pages 1–8. IEEE, 2018. 2
- [47] Joshua Robinson, Ching-Yao Chuang, Suvrit Sra, and Stefanie Jegelka. Contrastive learning with hard negative samples. *arXiv preprint arXiv:2010.04592*, 2020. 2
- [48] Nikolaos Sarafianos, Xiang Xu, and Ioannis A Kakadiaris. Deep imbalanced attribute classification using visual attention aggregation. In *Proceedings of the European Conference on Computer Vision (ECCV)*, pages 680–697, 2018. 6
- [49] Farzin Soleymani, Mohammad Eslami, Tobias Elze, Bernd Bischl, and Mina Rezaei. Deep variational clustering framework for self-labeling large-scale medical images. In *Medical Imaging 2022: Image Processing*, volume 12032, pages 68–76. SPIE, 2022. 1
- [50] Han Sungwon, Park Sungwon, Park Sungkyu, Kim Sundong, and Cha Meeyoung. Mitigating embedding and class assignment mismatch in unsupervised image classification. In *Proc. of European Conference on Computer Vision*, page 768–784, 2020. 2
- [51] Mohammad Reza Hosseinzadeh Taher, Fatemeh Haghighi, Michael B Gotway, and Jianming Liang. Caid: Context-aware instance discrimination for self-supervised learning in medical imaging. *arXiv preprint arXiv:2204.07344*, 2022. 1
- [52] Asher Trockman and J. Zico Kolter. Patches are all you need? 3
- [53] Asher Trockman and J Zico Kolter. Patches are all you need? *arXiv preprint arXiv:2201.09792*, 2022. 4, 5
- [54] Wouter Van Gansbeke, Simon Vandenhende, Stamatios Georgoulis, Marc Proesmans, and Luc Van Gool. Scan: Learning to classify images without labels. In *European conference on computer vision*, pages 268–285. Springer, 2020. 1, 2
- [55] Guangrun Wang, Keze Wang, Guangcong Wang, Philip HS Torr, and Liang Lin. Solving inefficiency of self-supervised representation learning. In *Proceedings of the IEEE/CVF International Conference on Computer Vision*, pages 9505–9515, 2021. 1, 4
- [56] Peng Wang, Kai Han, Xiu-Shen Wei, Lei Zhang, and Lei Wang. Contrastive learning based hybrid networks for long-tailed image classification. In *Proceedings of the IEEE/CVF conference on computer vision and pattern recognition*, pages 943–952, 2021. 6, 7

- [57] Junyuan Xie, Ross Girshick, and Ali Farhadi. Unsupervised deep embedding for clustering analysis. In *International conference on machine learning*, pages 478–487. PMLR, 2016. [1](#), [4](#)
- [58] Dejiao Zhang, Feng Nan, Xiaokai Wei, Shangwen Li, Henghui Zhu, Kathleen McKeown, Ramesh Nallapati, Andrew Arnold, and Bing Xiang. Supporting clustering with contrastive learning. *arXiv preprint arXiv:2103.12953*, 2021. [1](#), [4](#)
- [59] Richard Zhang, Phillip Isola, and Alexei A Efros. Colorful image colorization. In *European conference on computer vision*, pages 649–666. Springer, 2016. [2](#)